Chapter-5

DELINEATION AND MAPPING OF RIVERINE WETLANDS IN THE INTERFLUVES OF THE GANGA AND SAI RIVERS

5.1 Introduction

The interfluve of the Ganga and Sai Rivers has a tract of riverine wetlands, and it appears they are interconnected. These riverine wetlands are the hydrogeomorphic environmental unit of the Gangetic floodplain, but no work has been done with aspects of its geomorphological study and geological origin. Thus, it is necessary to keep a holistic approach and understanding of their hydro-geomorphological distribution and geological origins for any management plan for their conservation and restoration.

Therefore, this chapter aims to identify, delineate, and map the hydro-geomorphological features in the interfluvial zone of the Ganga and Sai Rivers.

5.2 Methodology

The remote sensing data (Satellite image and DEM) plays an indispensable role in discerning the riverine wetlands in the form of hydrogeomorphological features such as paleochannels, oxbow-lakes, meander scars, etc., (Rathore et al., 2010; Bhosle et al., 2009). Although the remote sensing data facilitates delineating these hydrogeomorphological features, it does not provide full confidence about the associated lost course alone. Thus, field observations, geophysical surveys (resistivity profiling) and sedimentary analysis are imperative for confirmation (Fitterman et al., 1991; Bhattacharyya et al., 2015; Resmi, et. al., 2017). After delineating the preserved abandoned river courses, the understanding of geomorphological history becomes an essential part. The flow chart of the methodology for this study is given in Fig. 5.1

5.2.1 Remote Sensing Data and Image Processing

The remote sensing data, i.e., Landsat 8 OLI (Operational Land Imager) satellite image, Shuttle Radar Topography Mission- Digital Elevation Model (SRTM- DEM) data and Sentinel image, downloaded from USGS, were used as primary data for the Delineation and extraction of the paleochannels of the study area. All the on-screen work in the GIS environment was performed using ERDAS Imagine-2014 and ArcGIS-10.6 software. For the digital image processing and enhancement of the image, techniques such as layer stacking, pan sharpening (hyperspherical colour space resolution merge), resampling pixel size, rescaling, histogram equalisation (enhancement of overall contrast in the image), colour composites and band combinations etc., were used. In the ERDAS IMAGINE software, using the resolution merge technique, panchromatic band and multispectral bands were merge and finally, a standard false-colour composite (FCC) Landsat-8 OLI satellite image with a spatial resolution of 15 m was prepared. The final image of Landsat-8 OLI (Fig. 5.2) and SRTM_DEM (Fig. 5.3) for the study area was generated by mosaicking three tiles of the Landsat-8 OLI satellite image and four tiles of the SRTM-DEM image, respectively.

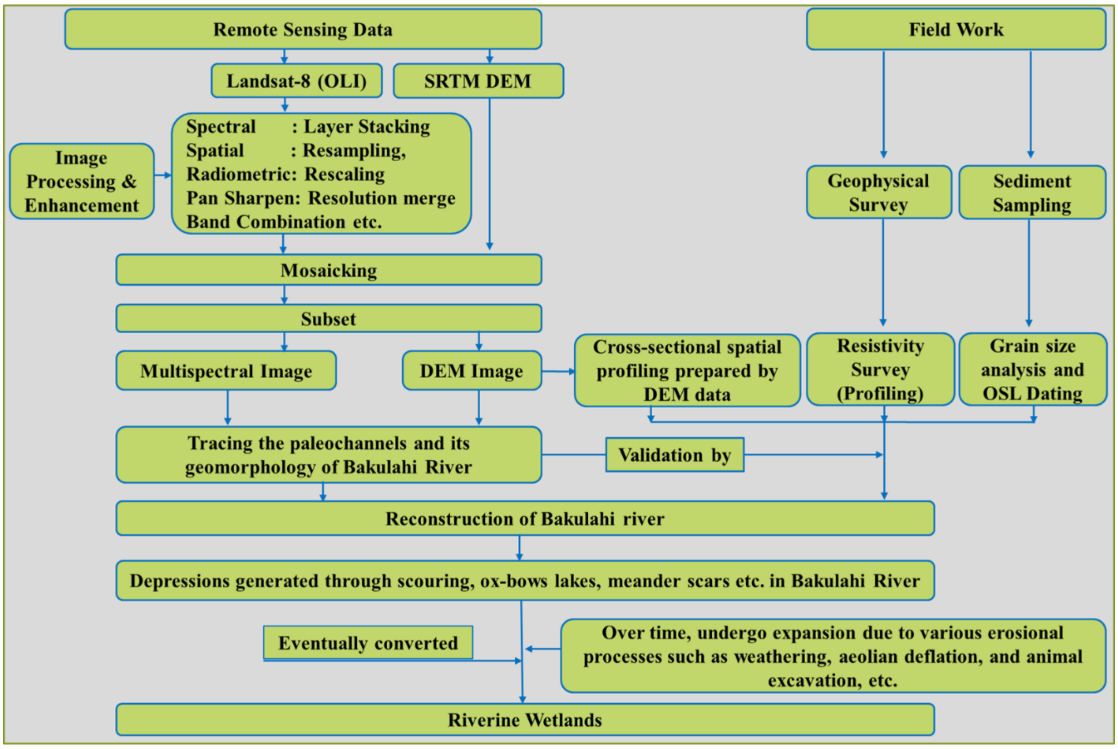

Fig. 5.1 Flow chart of the methodology.

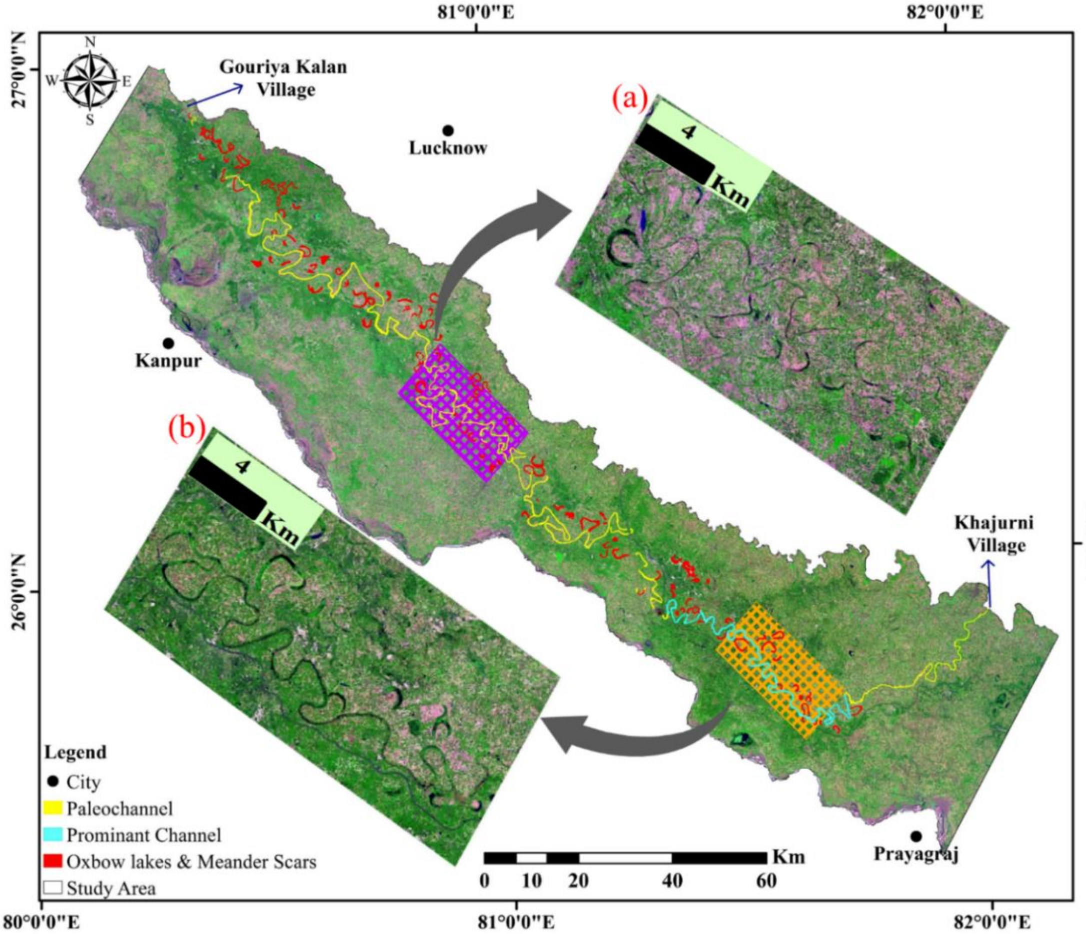

Fig. 5.2 False colour composite (FCC) image of Landsat 8 OLI bands 7, 5, 3 in RGB of the study area. The riverine wetlands in the form of paleochannels, prominent channels (channel filled with water whole year), ox-bow lakes and meander scars are denoted with yellow colour, cyan colour, and red colour, respectively. The zoomed image of the paleochannel (magenta-coloured hatched box) and prominent channel (orange-coloured hatched box) in the study are shown by (a) and (b), respectively.

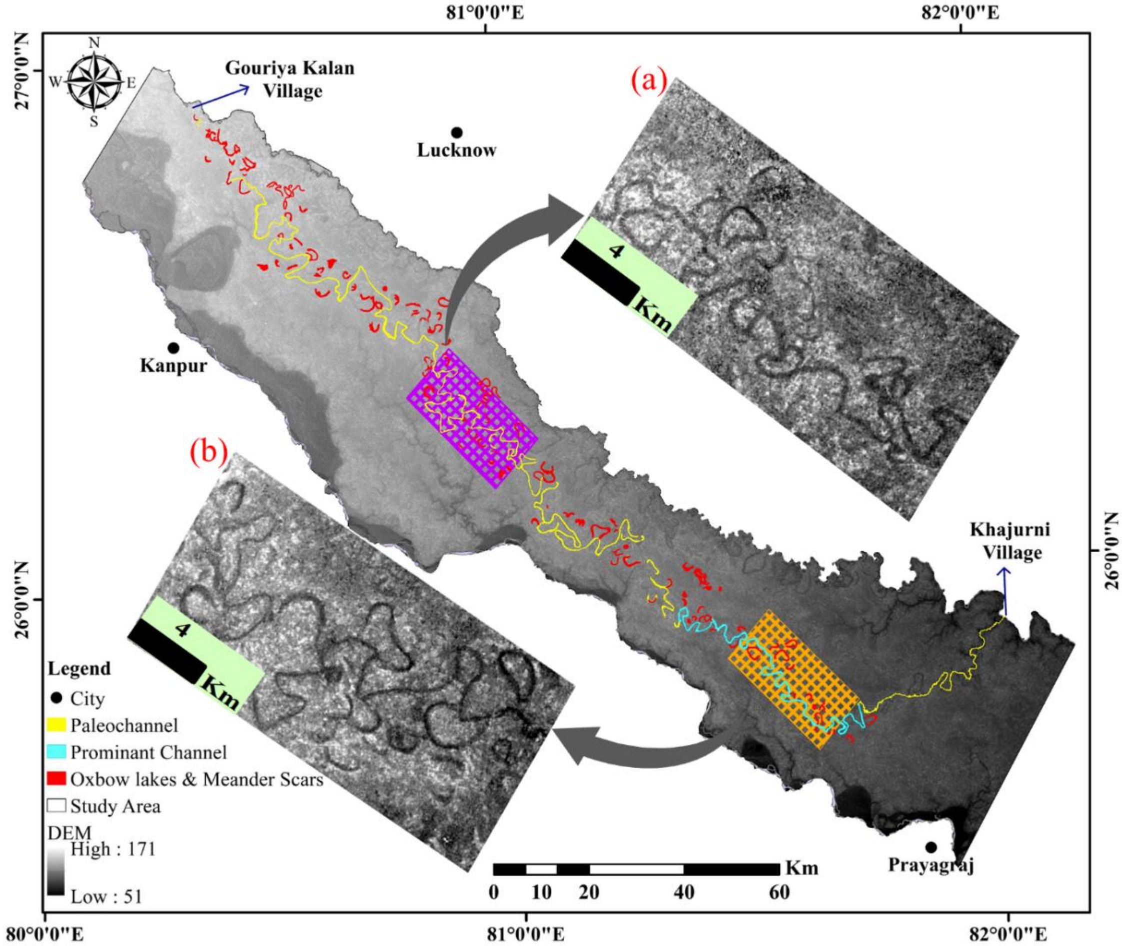

Fig. 5.3 SRTM DEM data also show continuous and properly interconnected paleochannel (yellow colour), prominent channel (cyan colour) and the series of associated ox-bow lakes and meander scar (red colour). The zoomed images ((a) and (b)) of the depressional feature of the paleochannel (magenta-coloured hatched box) and prominent channel (orange-coloured hatched box) are visualised in a dark tone.

5.2.2 Delineation of Riverine Wetlands

The hydro-geomorphological features (i.e., paleochannels, oxbow-lakes, meander scars, isolated lakes/ponds, etc.) are the primary signature of the riverine wetlands. The lensoidal/crescent-shaped forms, sinusoidal pattern, vegetation segments along these patterns, well- defined connectivity within these hydro-geomorphological features, and high reflectance in near-infrared (NIR) due to abundant vegetation play vital roles in identifying and delineating riverine wetlands (Fig. 5.2). Further, the delineated geomorphic features were cross-matched with the DEM image (Fig. 5.3). The different band combinations display the geomorphological features in different tones that may be taken as an identification marker of the riverine wetland (Sinha, et al. 2017b) (Fig 5.4 & Table 5.1). The riverine wetlands appear as a band of dark red tones in FCC (Band 5, 4, 3 on RGB) because of vegetation, which is a sign of sufficient moisture.

5.2.3 Spectral Indices

The spectral signatures of water and water-vegetation-associated features were used to identify and map the riverine wetlands (Szabo, et al. 2016; Suir and Sasser 2019; Liu, et al. 2014). Image-based indices, i.e., NDVI (Table 5.1, Eq. 1) and MNDWI (Table 5.1, Eq. 2), were generated using Landsat images in ERDAS IMAGINE 2014 software. MNDWI was used to identify water pixels, i.e., water bodies (McFeeters 1996; Fisher et al. 2016; Paul and Pal 2020), and NDVI was used to identify the aquatic vegetation (Taddeo et al. 2019; Eid et al. 2020). The values of NDVI and MNDWI range from -1 to 1 (Crippen 1990). Positive MNDWI values indicate water bodies, while 0 and negative values mark the terrestrial vegetation and soil. Negative NDVI values represent water, while positive values correspond to healthy vegetation (Crippen 1990; McFeeters 1996; Han-Qiu 2005; Pettorelli 2013).

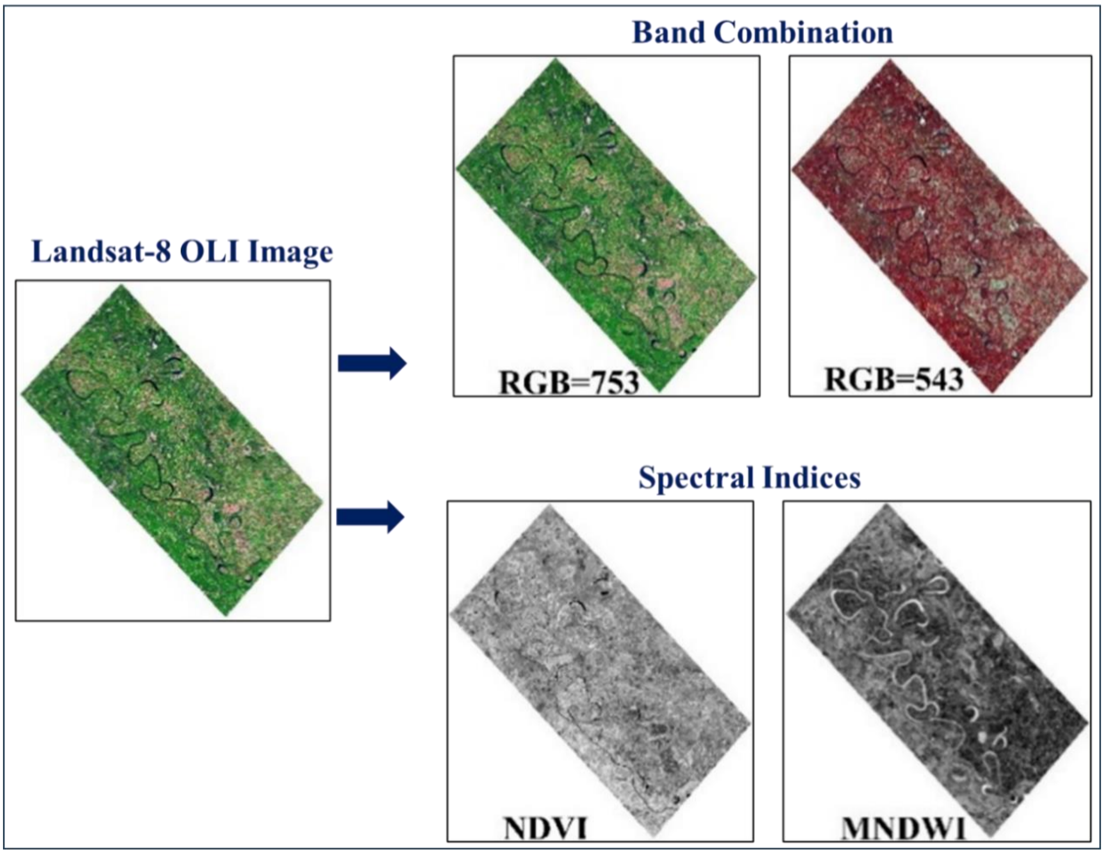

Fig. 5.4 Different band combinations in Landsat-8 (OLI) satellite image.

Table 5.1: Shows the different band combinations in Landsat-8 (OLI) satellite image and spectral indices.

Enhancement	Significance	
Band combinations	RGB (432)	Natural colour composites close to the true colour and replicates similar to humans can get through Landsat OLI image where green shows healthy vegetation, brown shows unhealthy flora, dark blue and black shows water, and grey and white show urban features.
	RGB (543)	False-colour composite is also known as near-infrared (NIR) composite. The band combination is very useful for examining vegetation because chlorophyll is a good reflector of near-infrared light. The red hue shows the area of healthy vegetation. Water is shown by dark areas and white, indicating urban areas.
	RGB (652)	This band combination can analyse agricultural crops. Where agriculture appears as a vibrant green colour and magenta show bare earth.
Spectral indices	NDVI	(NIR−Red)/(NIR+Red) …………………….(1)
	MNDWI	(Green−SWIR1)/(Green+SWIR1) …………(2)

5.2.4 Electrical Resistivity Survey

The resistivity of soil and rocks is highly susceptible to change with current due to the presence of water content. The electrical resistivity survey was carried out where the identification and delineation of riverine wetlands in the form of paleochannels were not confirmed using remote sensing. The electrical resistivity surveys are based on the assumption that subsurface geoelectric strata are isotropic and horizontally extended to infinite with distinct thickness and electrical resistivity (Dobrin and Savit, 1960; Yadav et al., 2010; Sinha et al., 2013). The resistivity meter (MODEL-SSR-MP1), a battery of 12 Volt, and four electrodes were used to observe the spatial extension of paleochannels. Profiling was done across the paleochannels at six sites (PL-1 to PL-6) (Fig 5.5) using the Wenner arrangement (Wenner 1916) along six transects, namely A-B, C-D, E-F, G-H, I-J, and K-L (Fig. 5.5). The two sites PL-1 and PL-2 (Fig. 5.6d) represent the detailed and zoomed picture of profiling near the origin sites of the river. A further cross-check also has been done by generating the spatial cross-sectional profiles of paleochannel in

Arc GIS 10.6 with the 3D analyst tool using SRTM DEM data along the same transect as resistivity profiling (A-B, C-D, E-F, G-H, I-J, and K-L) (Fig. 5.11).

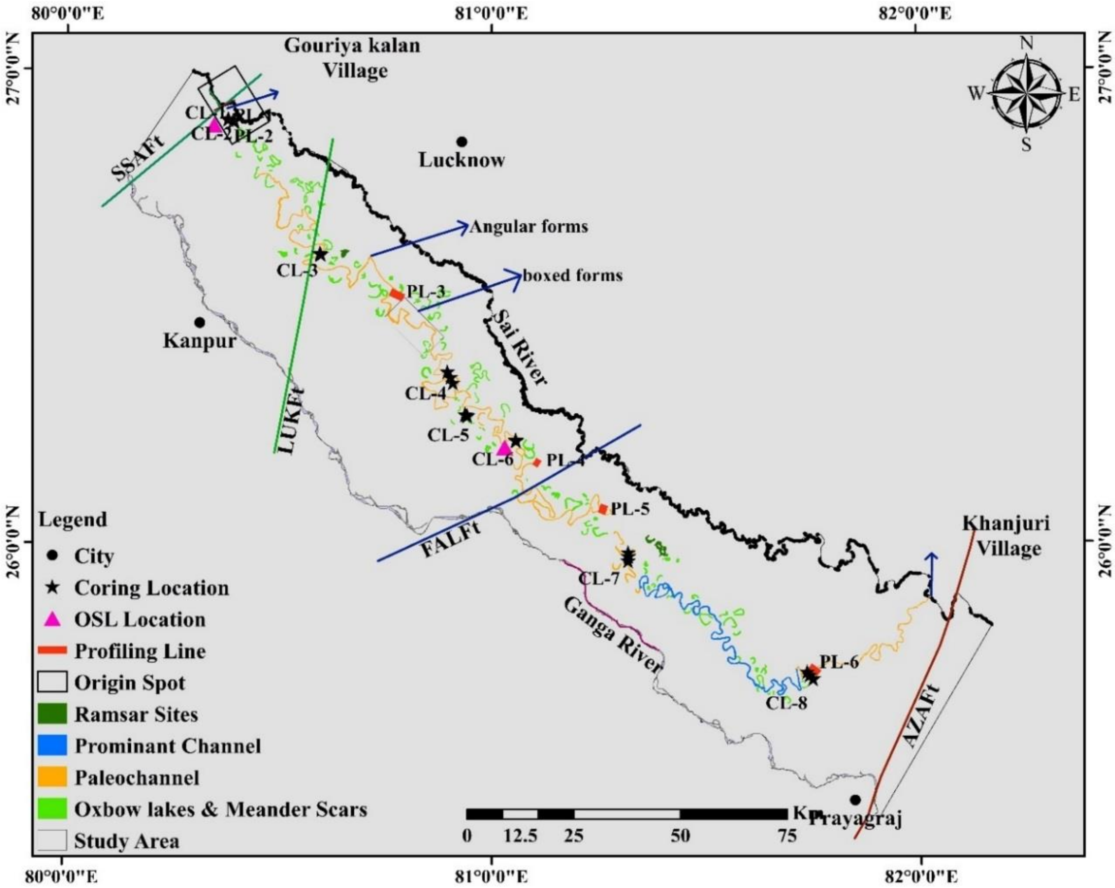

Fig. 5.5 The black rectangle at the northwest shows the first appearance of hydro-geomorphological features in the form of meanders. The blue, orange, and green lines show the prominent channels (called the Bakulahi River), the discontinuous Paleochannels and ox- bow lakes, respectively. Location of coring of samples (Black star), locations of cross-sectional profiling (Red line), location of sediments collected for Optical Stimulated Luminescence (OSL) dating (pink triangle) and the Sidhaur–Sandila Fault (SSAFt), Lucknow Fault (LUKFt), Faizabad–Lalganj Fault (FALFt), and Azamgarh–Allahabad Fault (AZAFt).

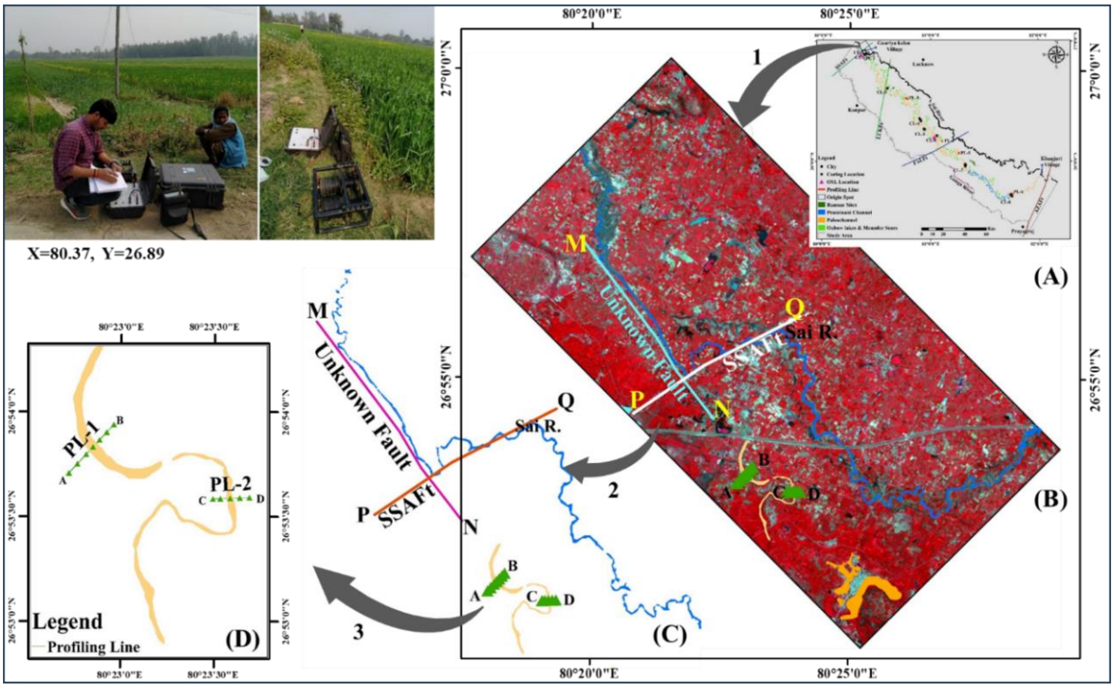

Fig. 5.6 (A) Arrow-1 Shows the spot from where the first meanders were observed. (B) the Sentinel satellite image shows the three times Sai River's course diversions at 90 degrees anticlockwise (U-turn). (C) Arrow-2 morphology of channel (D) first appearance of isolated meanders, where resistivity survey was carried out to decipher the hydro-geomorphological features.

5.2.5 Sedimentological Analysis

Sedimentological studies such as grain size analysis were helpful in tracing the channel belts, which were otherwise not identified through remote sensing images. The proportion of channel fills and mean grain size of channel fills relative to lateral-accretion deposits also help in locating the paleochannels (Bridge 1985; Guccione 1993). Flow regimes with high energy sustain coarser sediments, while the finer sediments are found in the low energy flow regime (Friedman 1962; Folk 1966). Therefore, relatively coarser sediments are found in the channel belts and fine sediments on the overbank of the alluvial deposits (Allen 1965, 1978). Further analysis of grain size distribution provides detailed information about the sediments, which in consequence, predicts the depositional environments (Folk and Ward 1957).

For tracing the belts of channels, sediment samples were collected from eight sites (CL-1 to CL-8) (Fig. 5.5) across the paleochannel. From each site, representative samples were collected from all three locations (left bank, middle and right bank) of the channel with the closed bucket soil auger of 9 cm diameter at a depth of 60 cm to 150 cm. Before sampling, the ground was scraped carefully, and the top litter layer was removed. Three to four kilograms of representative samples with their duplicates were collected safely and carried in air-tight poly- bags to the laboratory and analysed. In the laboratory, sieve analysis and hydrometer tests were conducted for each of the samples following the IS (Indian Standard) code 2720 (Part 4) 1985. In sieve analysis, with the help of a sediment shaker, sediments were passed through sieves of 5.6 mm, 4.0 mm, 2.0 mm, 1mm, 0.425 mm, 0.250 mm, 0.125 mm, 0.075 mm (Fig. 5.7B). The sediments finer than 0.075 mm were analysed by the hydrometer test (Fig. 5.7C). The percentage of gravel, sand, silt and clay for each sample has been calculated and plotted in USDA soil texture triangular diagram (Fig. 5.8). The various statistical parameters such as mean, sorting, skewness and kurtosis were determined for the analysis of the depositional environment using the following formula (Folk and Ward 1957).

Mean $= (\Theta_{16} + \Theta_{50} + \Theta_{84})/3.$

Sorting $= \{(\Theta_{84} - \Theta_{16})/4 + (\Theta_{95} - \Theta_{5})/6.6\}.$

Skewness $= [\{(\Theta_{16} + \Theta_{84} - 2\Theta_{50})/2(\Theta_{84} - \Theta_{16})\}] + [\{(\Theta_{5} + \Theta_{95} - 2\Theta_{50})/2(\Theta_{95} - \Theta_{5})\}]$

Kurtosis $= \{(\Theta_{95} - \Theta_{5})/2.44(\Theta_{75} - \Theta_{25})\}$

Where Θ_x refers to grain size at the x percentile on the cumulative grain size curve.

In sedimentology, the mean represents the average particle size in a sediment sample, calculated using the arithmetic mean. Sorting indicates the uniformity of particle sizes, with well-sorted sediments having a narrow size range and poorly sorted ones having a wide range. Skewness measures the asymmetry in the distribution, with positive skewness indicating more fine-grained particles and negative skewness indicating more coarse-grained particles. Kurtosis reflects the tailedness of the distribution, with mesokurtic, leptokurtic, and platykurtic distributions describing the peak's shape. These statistical parameters provide insights into sediment characteristics and depositional processes, aiding in the interpretation of sedimentary environments and geological history.

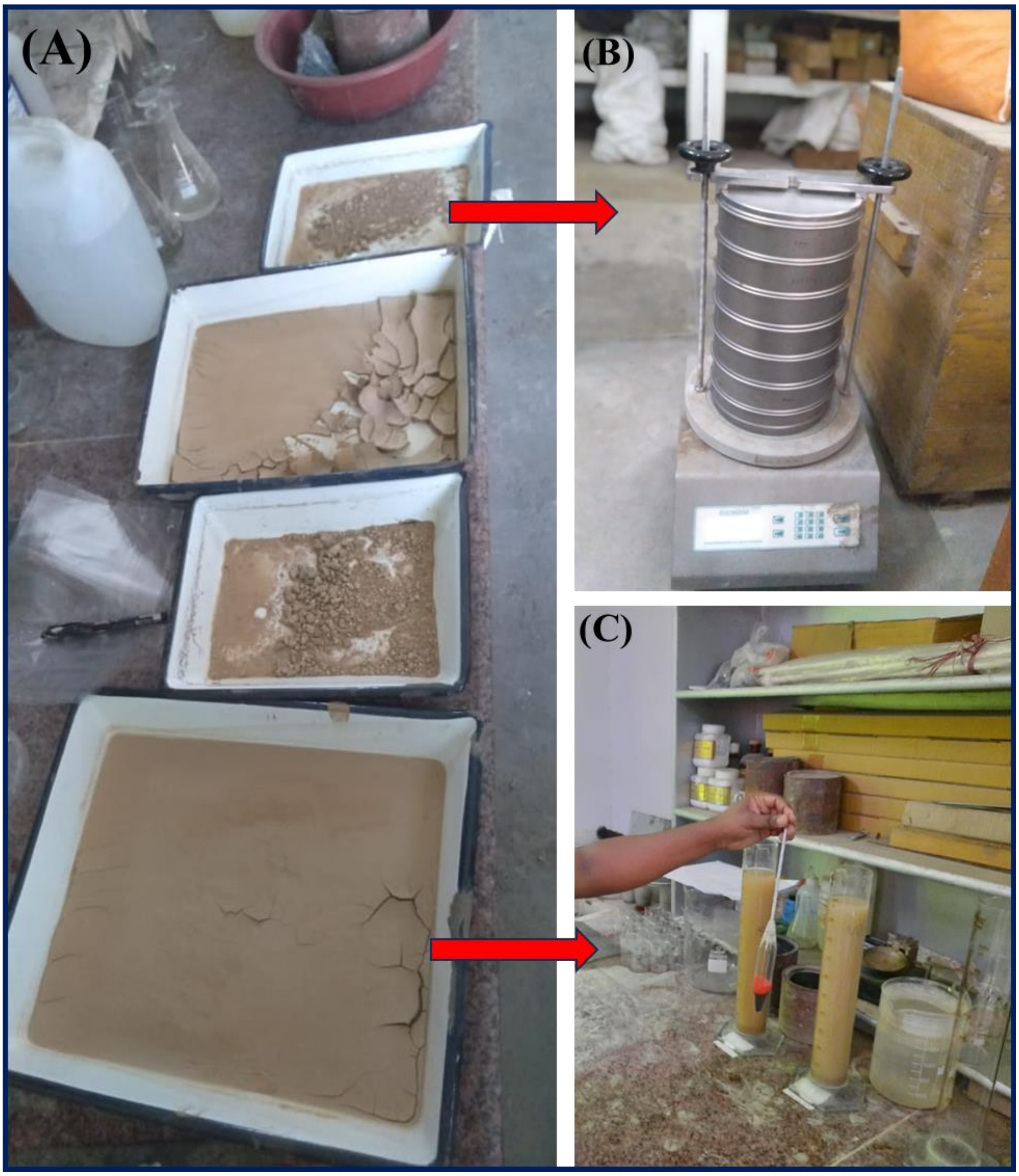

Fig. 5.7 Photographs show the lab instrument for sieve analysis. (A) Separated sediments in trey for sieve analysis and hydrometer test. (B) The upper arrow shows the grains greater than 0.075 mm passes through sieves of 5.6 mm, 4.0 mm, 2.0 mm, 1mm, 0.425 mm, 0.250 mm, 0.125 mm, 0.075 mm. (C) The lower arrow shows the grains less than 0.075 mm were done by hydrometer test.

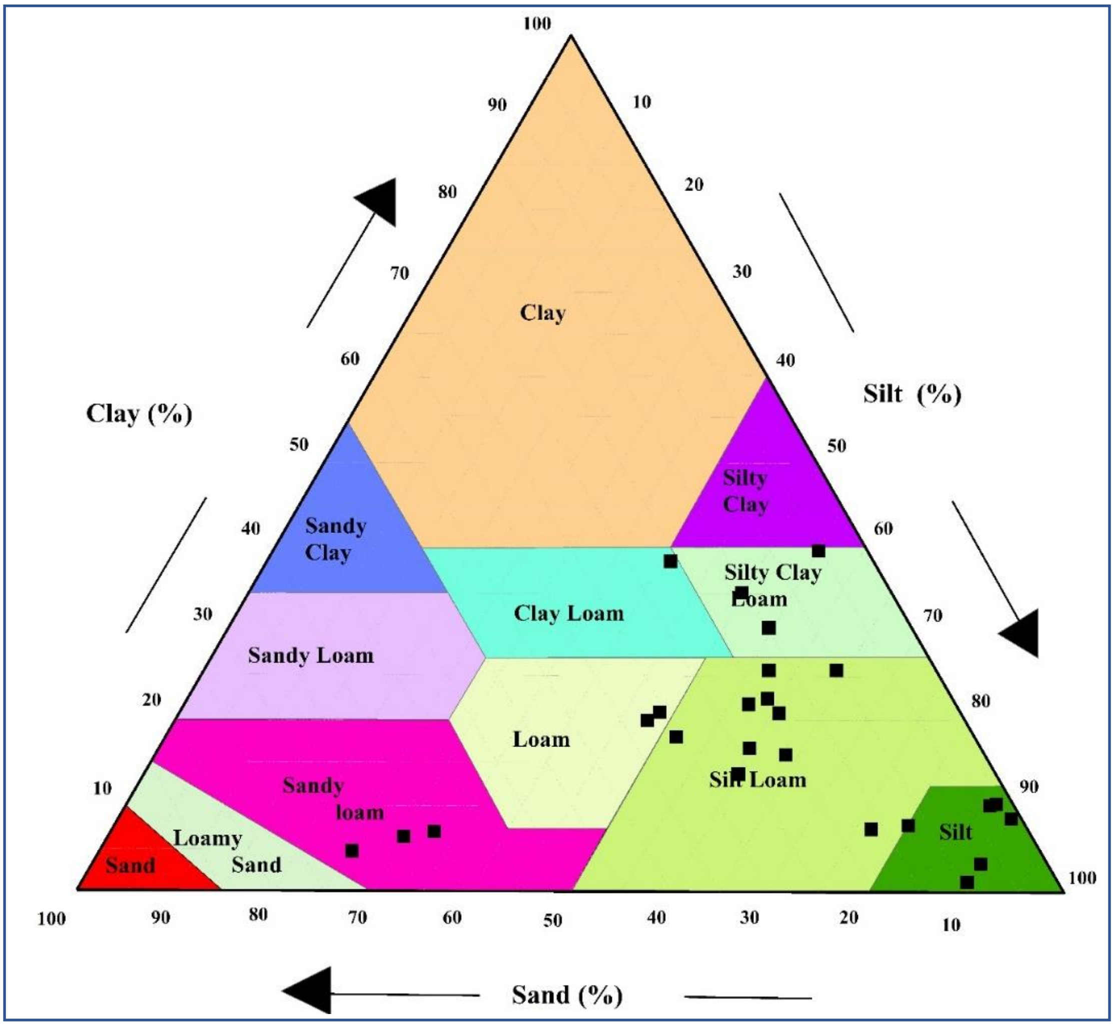

Fig. 5.8 Classification of soil texture of samples from the study area as per USDA soil texture triangular diagram

5.2.6 Hydro-geomorphological analysis

Meanders are the most recognisable geomorphic features of the alluvial landscape. The geomorphology changes in a river can be understood by the meandering process and geomorphological parameters such as sinuosity, wavelength, amplitude and number of meanders. Sinuosity is defined as the deviation in a channel from its straight-line course. The Sinuosity Index is calculated as the ratio of the channel length (Lc) to the valley length (Lv) (Mueller 1968). The higher sinuosity value indicates the river's instability with a high proportion of suspended loads (Schumm 1972, 1977). The migration rate of a meandering river is positively correlated with the bend tightness index. The bend tightness index is defined as how tightly or loosely a river has bends. It is calculated as the ratio of the radius of curvature to the mean channel width of a meander (Bag et al., 2019). The angle of curvature is the angle at the centre that corresponds to the arc length of a circle that fits the meandering arc. The radius of curvature (Rc) is measured by the radius of a circle that fits the meandering arc from the outside of the bank-full channel to the crossing point of two lines that perpendicularly bisect the tangent lines of each meander departure point (Nimnate et al. 2017). The average width of each mapped meander was measured by taking the mean of three cross-sectional lengths near the inflexion point. The higher the tightness index values, the higher the rates of bend migration.

The geomorphic parameters of paleochannels and prominent channels (channel filled with water whole year) were worked out in Arc GIS 10.6. For convenient calculation of geomorphological parameters, the whole tract of the interfluvial zone is divided into Reach-1, Reach-2, Reach-3 and Reach-4 (Fig 5.9). Valley length and channel length were measured, and sinuosity for each reach was calculated (Table 5.4). The average sinuosity was calculated by taking the mean of the sinuosity index of four reaches. The total number of meanders was calculated. Three prominent meanders from each reach were selected (Fig. 5.10) to measure the average width, radius of curvature, angle of curvature and bend tightness index.

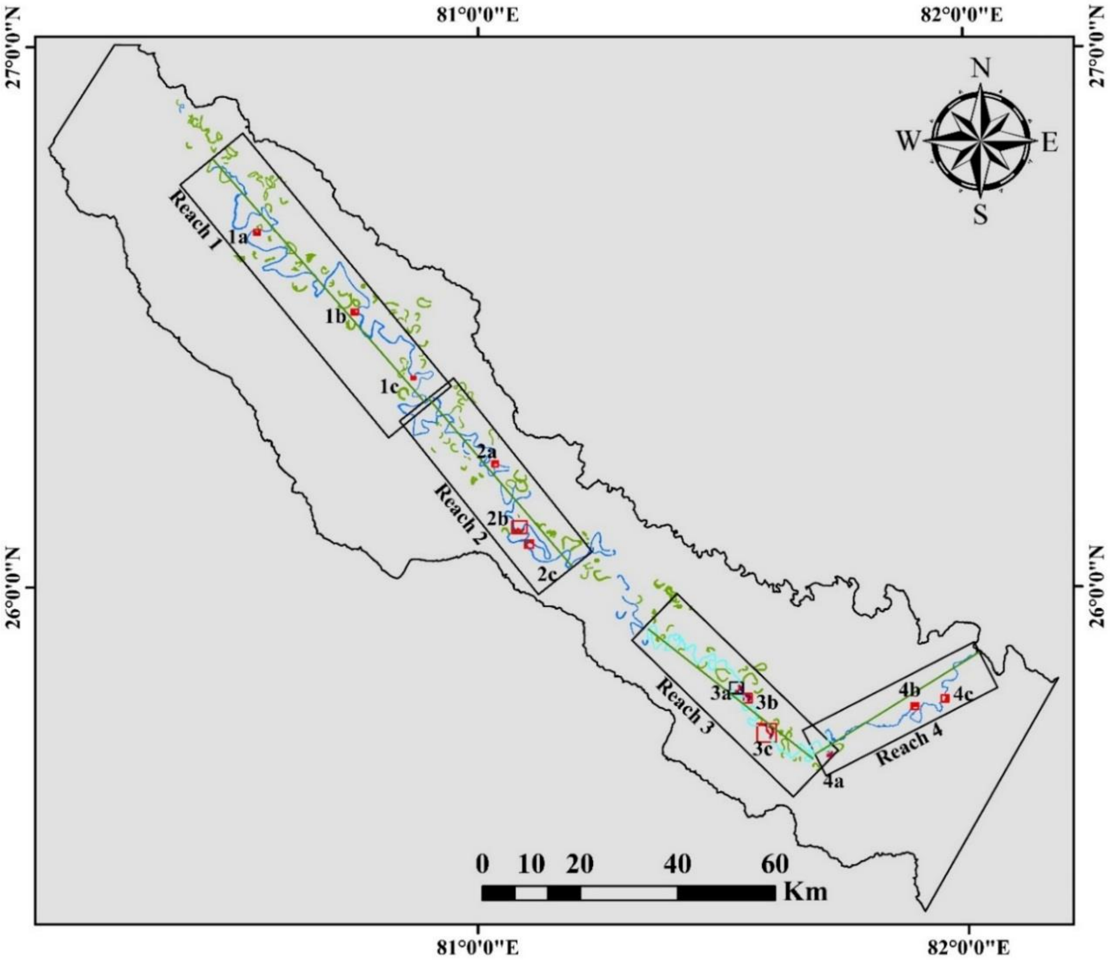

Fig. 5.9 Study area is divided into four reaches (Reach-1, Reach-2, Reach-3, Reach-4). Meanders in red coloured boxes in each reach (Reach-1(1a,1b,1c), Reach-2 (2a,2b,2c), Reach- 3(3a,3b,3c), and Reach-4 (4a,4b,4c)) shows the selected meanders for calculation of geomorphological parameters.

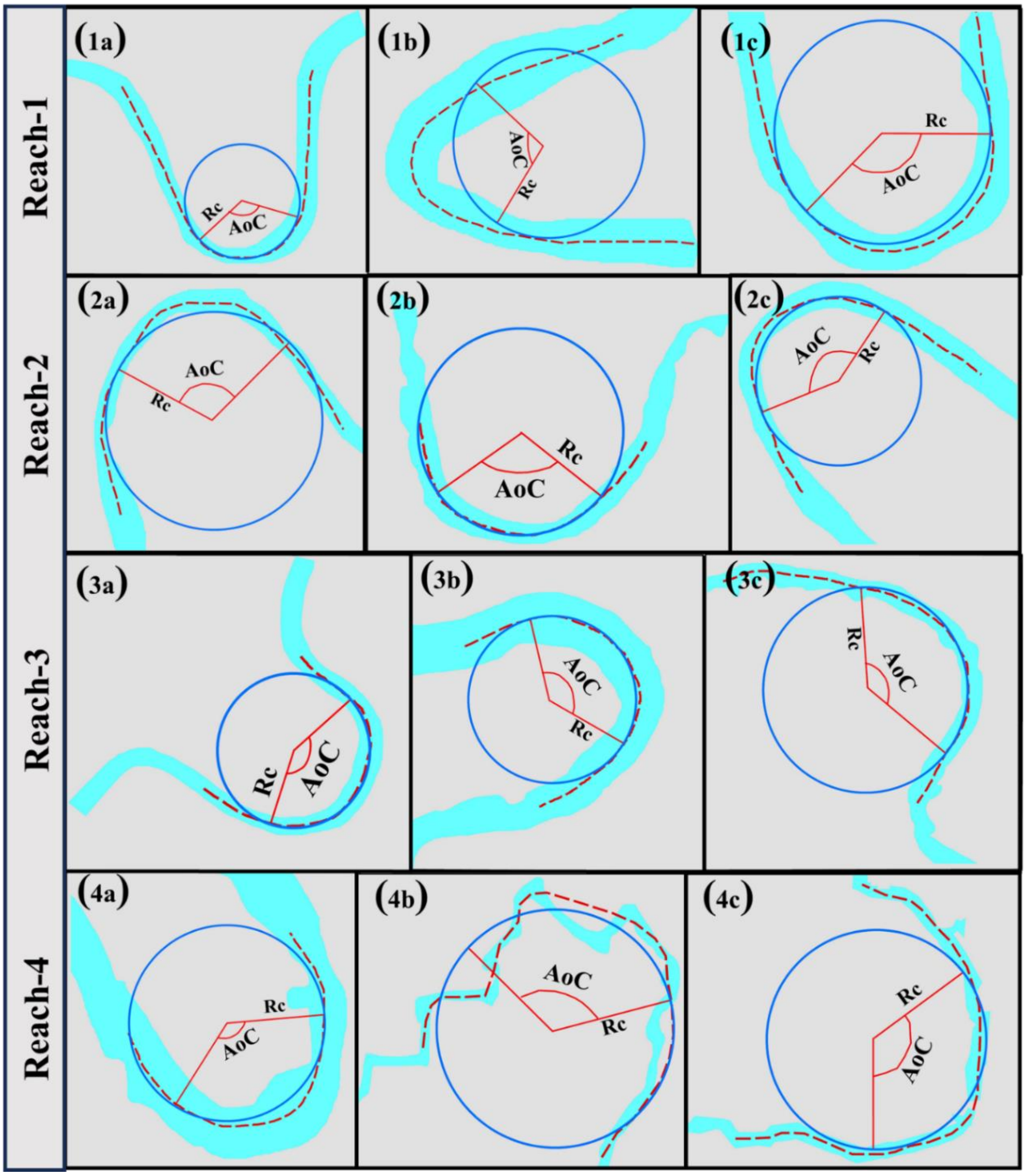

Fig. 5.10 Meanders selected from Reach-1(1a,1b,1c), Reach-2 (2a,2b,2c), Reach-3(3a,3b,3c), and Reach-4 (4a,4b,4c). Rc = radius of curvature and AoC = angle of curvature.

5.2.7 Optically Stimulated Luminescence (OSL) dating

The luminescence dating technique is based on the time of last exposure of quartz and feldspar minerals to light. The OSL signal is susceptible to light; therefore, it is used for the dating of fluvial sediments (Aitken 1998). The dating of sediments from the channel is very helpful in knowing the time of flowing condition of the river (Srivastava et al., 2003). Samples for OSL dating were collected in opaque galvanised iron (GI) pipes from two sites (Pink triangle in Fig. 5.5) in the study area. A photograph of sampling for OSL dating has been given (Fig. 11(F)). The collected samples were sent to the TL/OSL (thermoluminescence and Optically Stimulated Luminescence) Laboratory, Wadia Institute of Himalayan Geology (WIHG), Dehradun, Uttarakhand, India, for OSL dating.

5.3 Result

5.3.1 Delineation of Paleochannels

A series of hydro-geomorphological features (i.e., numerous sinuous underfit rivers, traces of channels with continuous or discontinuous segments, associated ox-bow lakes and meander scars) have been identified and delineated in the Landsat-8 OLI, FCC image (Band 7, 5, 3 on RGB) in the upper reaches of the currently flowing Bakulahi river (just after Gouria Kalan village near Bangarmau in Unnao district) in the interfluvial zone of the Ganga and Sai Rivers (Fig. 5.2). These hydro-geomorphological features are shown as dark tone in the SRTM DEM map (Fig. 5.3), and superimposing with the hydro-geomorphological features delineated in the Landsat-8 OLI image. These hydro-geomorphological features have characteristic morphology. They exhibit successive lateral shifting and complex looping. The general alignments of sub-harmonic meander orientations are suggestive of their past continuity. The stream course/features in the interfluvial tract can be apparently divided as prominent and continuous channels and discontinuous traces of the channel. In maximum parts of the interfluvial zone, discontinuous traces of channels (paleochannels) are present (orange- coloured stream in fig. 5.5), while in some parts, prominent and continuous channels (blue- coloured stream in fig. 5.5) are present. Although in the prominent and continuous channels, water is present only during the rainy season. In the upper tract of the interfluvial zone, from Gauriya Kalan village, Bangarmau (Unnnao) to Uchhahar (Raebareli), for a length of approximately 408km, there is only discontinuous traces of channels are present (orange- coloured stream in fig. 5.5). From Uchhahar (Raebareli) to Azad Nagar (Pratapgarh), for a length of about 85 km, physically continuous and prominent channel is present, currently referred as Bakulahi River (blue-coloured stream in Fig. 5.5). After Azad Nagar (Pratapgarh), again discontinuous traces of channels are present (orange-coloured stream in Fig. 5.5) in the lower tract. These channel segments are poorly visible as they lose their continuity in alluvium and appear to advance toward the northward direction and terminate at the confluence with Sai River at Khajurni village in the Pratapgarh district.

5.3.2 Resistivity Data

The electrical resistivity profiling (Wenner array) at six sites (PL-1 to PL-6) (Fig. 5.5) along the transect A-B, C-D, E-F, G-H, I-J, and K-L (Fig. 5.11) has been carried out, keeping the electrode at a distance of 5 meters. In order to ascertain the uppermost recognisable point/locality of the beginning of the river in question, two cross-sectional resistivity profiling near Asarfabad village and near Dholwa village were carried out along sections A-B in the NE- SW direction and sections C-D in the E-W direction (Fig. 5.6D). Indeed, the area had the first appearance of two isolated meanders, and it was important to decipher if they belonged to the same continuous channels. Observing the first site (PL-1), along transect A-B, across the channel, there is a variation in the resistivity value. The A-B transect is 205 m, measuring across the partially exposed channel. The value of resistivity gradually decreases from point A, which reaches a minimum value at a distance of 60m to 110m and then increases up to point B (Fig. 5.11(A-B)). The second site (PL-2), along transect C-D (205m), also shows the same trend of resistivity profiling; over the distance between 90 to 160 meters from point C and then increases up to point D (Fig. 5.11(C-D)). The decrease in resistivity value is due to the presence of moisture condition. The presence of moisture reveals that paleochannels are present between 60 meters to 110 meters along transect A-B from point A and between 90 meters to 160 meters along transect C-D, respectively. The resistivity profiling from the other four locations (E-F, G-H, I-J, and K-L) also shows similar trends as PL-1 and PL-2 (Fig. 5.11) and Table 5.2.

The symmetrical and asymmetrical U-shaped or V-shaped shaped topographic cross-sectional profiles generated from SRTM DEM data along same transection A-B, C-D, E-F, G-H, I-J, and K-L (same as resistivity profiling) (Fig. 5.11) also support in the confirmation of the presence of paleochannels.

Table 5.2 Shows the electrical resistivity profiling (Wenner array) value at six sites, i.e., PL-1, PL-2, PL-3, PL-4, PL-5, and PL-6.

		PL-1	PL-2	PL-3	PL-4	PL-5	PL-6
		X=80.38 DD	X=80.39 DD	X=80.78 DD	X=81.11 DD	X=81.26 DD	X=81.75 DD
		Y=26.90 DD	Y=26.89 DD	Y=26.53 DD	Y=26.17 DD	Y=26.07 DD	Y=25.73 DD
Sr. No.	Length	ρ (Ω·m)	ρ (Ω·m)	ρ (Ω·m)	ρ (Ω·m)	ρ (Ω·m)	ρ (Ω·m)
1	15	37.21	48.01	46.85	44.33	27.00	25.53
2	25	24.41	42.98	45.51	43.09	22.53	25.95
3	35	33.20	32.81	37.02	39.02	19.63	23.29
4	45	27.32	31.10	35.53	27.77	21.54	20.85
5	55	29.36	40.60	33.37	24.46	25.34	29.77
6	65	30.00	32.95	34.01	28.85	22.62	36.42
7	75	21.19	33.57	22.13	28.25	25.25	38.06
8	85	21.14	33.03	24.96	19.40	20.50	48.80
9	95	21.69	33.91	18.92	20.35	22.84	44.95
10	105	30.85	22.48	19.98	21.35	30.72	48.83
11	115	32.69	21.41	21.30	20.41	28.61	
12	125	43.09	27.40	30.19	22.37	32.03	
13	135	42.93	20.66	31.14	30.14	31.58	
14	145	46.41	25.08	31.94	26.69	34.74	
15	155	43.69	24.02	35.23	39.12	34.05	
16	165	45.04	47.28	38.60	38.39	34.67	
17	175	39.11	52.34	32.81	54.76		
18	185	40.46	50.39	34.29	52.54		
19	195	40.53	45.85	49.77	53.68		
20	205	36.20	53.38	51.97	39.12		

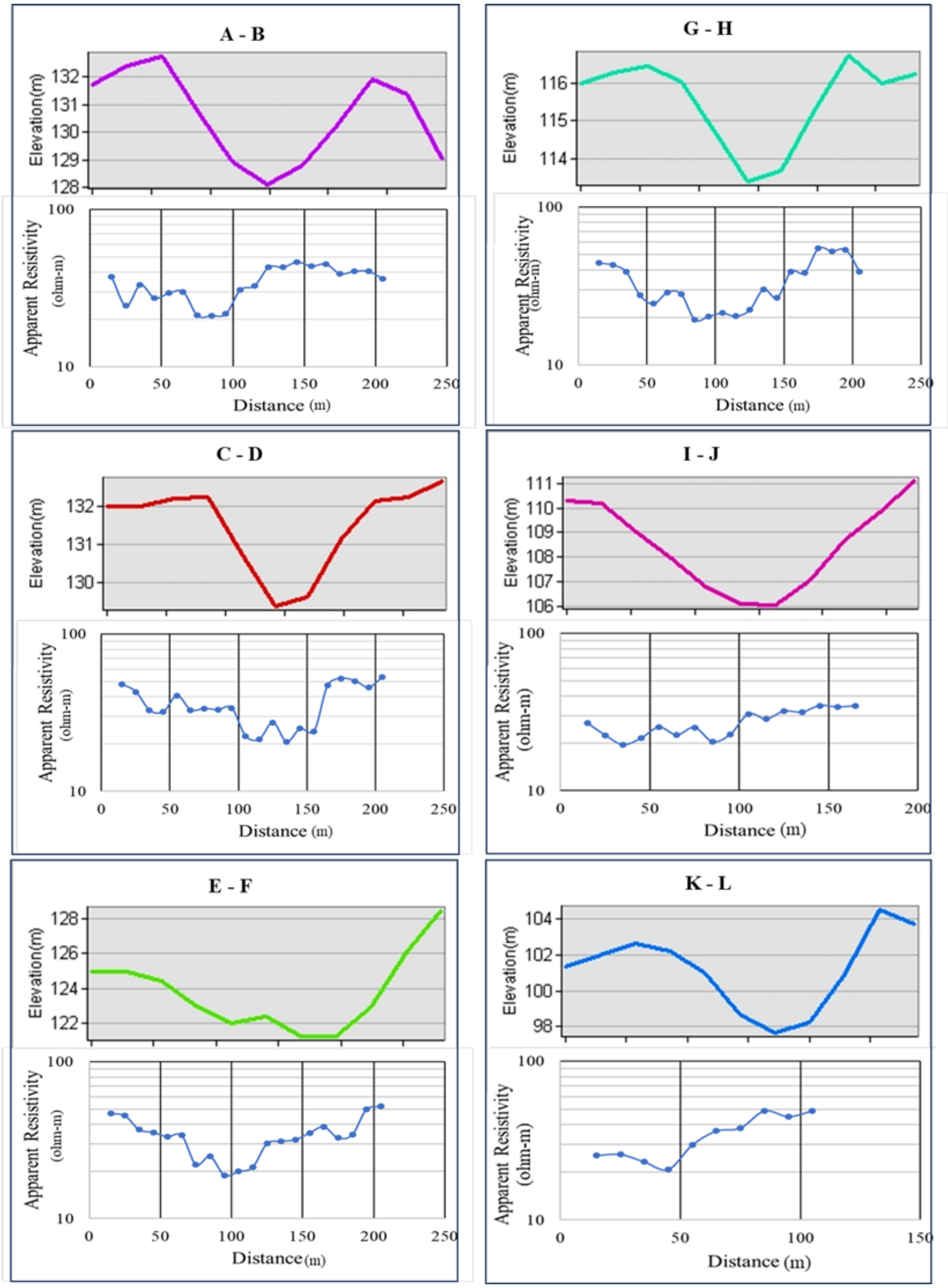

Fig. 5.11 The electrical resistivity profiling across the paleochannel at six sites (Wenner array) and corresponding topographic spatial cross-sectional profile using SRTM DEM data along the same line as the electrical resistivity profiling.

5.3.3 Grain Size Analysis

The result of the grain size analysis of samples collected from eight sits (CL-1 to CL-8) and various statistical parameters such as mean, sorting, skewness, and kurtosis were calculated in Table 5.3 and shown in Fig 5.12. The percentage of gravel, sand, silt, and clay in each sample is plotted in USDA soil texture triangular diagram (Fig. 5.8), which represents that the sediment deposits belong to silt loam, silty clay loam and silt in nature. The sedimentological archive from site-1, site-2, site-3, and site-7 show that considerably coarser grains are deposited in the left and right banks of the channel. Whereas the central part of the channel receives a significantly higher amount of silt, which shows an active flow regime of the channel. These flow conditions show that the sand was deposited in the higher flow region of the channel, probably during the last flooded condition. The regime of the channel gradually changes, and it shifts toward the lower flow condition, which deposits silt and clay in the central part. Other samples collected from site-4, site-5, site-6 and site-8 show a higher percentage of silt and sand in the mid-channel, whereas side channels receive a skewed distribution of grains.

Table 5.3 Shows the result of the grain size analysis and its description

Site Name	Latitude (DD)	Longitude (DD)	Gravel (%)	Sand (%)	Silt (%)	Clay (%)	Mean	Sorting	Skewness	Kurtosis	Description
Site-1 Left bank (l=30-60cm)	26.58	80.62	0.00	21.17	63.68	15.15	0.05	0.07	0.00	1.50	Coarse sand, very well sorted, symmetrical, very leptokurtic
Site-1Left bank (l=60-90cm)	26.58	80.62	0.00	30.56	51.67	17.77	0.06	0.05	0.00	0.77	Coarse sand, very well sorted, symmetrical, Platykurtic
Site-1 Mid Channel (l=30-60cm)	26.58	80.62	0.00	1.23	87.66	11.11	0.04	0.03	-1.00	0.00	Coarse sand, very well sorted, very coarse skewed, very platykurtic
Site-1 Mid Channel (l=60-90)	26.58	80.62	0.30	1.71	86.73	11.26	0.04	0.02	-1.00	0.00	Coarse sand, very well sorted, very coarse skewed, very platykurtic
Site-1 Mid Channel (l=90-120cm)	26.58	80.62	0.07	1.79	89.80	8.34	0.03	0.03	0.90	-0.46	Coarse sand, very well sorted, very fine skewed, very platykurtic
Site-1 Right bank (l= 50-60cm)	26.58	80.62	6.78	8.18	83.77	1.27	0.04	0.03	-1.00	0.00	Coarse sand, very well sorted, very coarse skewed, very platykurtic
Site-1 Right bank (l=100cm)	26.58	80.62	2.58	6.71	88.45	2.26	0.04	0.17	-0.05	0.00	Coarse sand, very well sorted, symmetrical, very platykurtic
Site-2 Left bank (l=60-90cm)	26.89	80.39	0.00	18.47	60.75	20.78	0.03	0.04	0.55	0.88	Coarse sand, very well sorted, very fine skewed, Platykurtic
Site-2 Mid Channel (l=60-90cm)	26.89	80.39	1.50	12.70	77.60	8.20	0.04	0.03	0.73	0.85	Coarse sand, very well sorted, very fine skewed, Platykurtic
Site-2 Right bank (l=60-90cm)	26.89	80.39	0.00	22.20	55.40	22.40	0.05	0.05	0.84	0.98	Coarse sand, very well sorted, very fine skewed, Mesokurtic
Site-3 Left bank (l=30-60cm)	26.61	80.60	6.73	16.15	70.18	6.94	0.07	0.89	0.71	0.00	Coarse sand, moderately sorted, very fine skewed, very platykurtic
Site-3 Left bank (l=60-90cm)	26.61	80.60	0.44	12.46	79.04	8.06	0.05	0.04	-0.45	0.00	Coarse sand, very well sorted, very coarse skewed, very platykurtic
Site-3 Mid channel (60-90 cm)	26.61	80.60	0.22	4.18	55.83	39.77	0.01	0.01	0.91	1.62	Coarse sand, very well sorted, very fine skewed, very leptokurtic
Site-3 Right bank (60-90cm)	26.61	80.60	2.08	10.20	63.16	24.56	0.02	0.08	0.70	3.04	Coarse sand, very well sorted, very fine skewed, extremely leptokurtic
Site-3 Right bank (90-120cm)	26.61	80.60	11.95	13.40	47.18	27.47	0.67	0.50	0.00	0.00	Coarse sand, well sorted, symmetrical, very platykurtic
Site-4 Left bank (l=100cm)	26.35	80.90	3.25	15.96	47.18	33.61	0.03	0.32	0.81	16.66	Coarse sand, very well sorted, very fine skewed, extremely leptokurtic
Site-4 Left bank (l=120cm)	26.35	80.90	9.81	17.67	52.80	19.72	0.15	0.11	0.00	0.00	Coarse sand, very well sorted, symmetrical, very platykurtic
Site-4 Mid Channel (l=100cm)	26.35	80.90	0.09	32.98	46.59	20.34	0.05	0.07	0.62	0.83	Coarse sand, very well sorted, very fine skewed, platykurtic
Site-4 Right bank (l=100cm)	26.35	80.90	17.96	51.70	24.76	5.58	1.65	1.21	0.00	0.00	Medium sand, poorly sorted, symmetrical, very platykurtic
Site-4 Mid Channel (l=120cm)	26.35	80.90	0.74	31.18	47.39	20.69	0.05	0.05	0.51	0.41	Coarse sand, very well sorted, very fine skewed, very platykurtic

Site Name	Latitude (DD)	Longitude (DD)	Gravel (%)	Sand (%)	Silt (%)	Clay (%)	Mean	Sorting	Skewness	Kurtosis	Description
Site-5 Left bank(l=100cm)	26.27	80.94	3.77	16.62	55.41	24.20	0.05	0.48	0.91	22.83	Coarse sand, well-sorted, very fine skewed, extremely leptokurtic
Site-5 Mid Channel (l=100cm)	26.27	80.94	29.80	18.62	41.68	9.90	0.02	0.00	0.00	0.00	Coarse sand, very well sorted, symmetrical, very platykurtic
Site-5 Mid Channel (l= 120cm)	26.27	80.94	28.17	31.29	26.92	13.62	0.14	0.00	0.00	0.00	Coarse sand, very well sorted, symmetrical, very platykurtic
Site-5 Right bank (l=100cm)	26.27	80.94	4.00	20.64	42.11	33.25	0.05	0.64	0.88	41.71	Coarse sand, moderately well-sorted, very fine skewed, extremely leptokurtic
Site-6 Left bank (100cm)	26.22	81.05	0.17	69.45	25.04	5.34	0.09	0.07	-0.50	1.49	Coarse sand, very well sorted, very coarse skewed, Leptokurtic
Site-6 Mid Channel (l=100cm)	26.22	81.05	0.74	21.24	41.20	36.82	0.04	0.10	0.94	5.14	Coarse sand, very well sorted, very fine skewed, extremely leptokurtic
Site-6 Mid Channel (l=120cm)	26.22	81.05	26.58	44.00	24.72	4.70	0.05	0.00	0.00	0.00	Coarse sand, very well sorted, symmetrical, very platykurtic
Site-6 Village side (100cm)	26.22	81.05	2.96	21.80	58.39	16.85	0.05	0.18	0.81	5.57	Coarse sand, very well sorted, very fine skewed, extremely leptokurtic
Site-7 Left bank (l=100cm)	25.97	81.31	2.35	25.87	57.68	16.46	0.06	0.06	0.00	1.13	Coarse sand, very well sorted, symmetrical, leptokurtic
Site-7 Mid Channel (l=100cm)	25.97	81.31	0.12	1.58	88.07	10.24	0.04	0.03	-0.37	-0.15	Coarse sand, very well sorted, very coarse skewed, very platykurtic
Site-7 Mid Channel (l=120cm)	25.97	81.31	0.09	1.88	85.43	10.56	0.03	0.03	1.20	-0.85	Coarse sand, very well sorted, very fine skewed, very platykurtic
Site-7 Right bank (l=100cm)	25.97	81.31	4.68	7.45	86.11	1.77	0.04	0.10	-0.53	0.00	Coarse sand, very well sorted, very coarse skewed, very platykurtic
Site-8 Left bank (l=100cm)	25.70	81.72	6.53	16.82	49.99	26.67	0.09	0.21	0.41	8.33	Coarse sand, very well sorted, very fine skewed, extremely leptokurtic
Site-8 Mid Channel (l=100cm)	25.69	81.73	0.42	32.08	46.99	20.52	0.05	0.06	0.56	0.62	Coarse sand, very well sorted, very fine skewed, very platykurtic
Site-8 Mid Channel (l=120cm)	25.69	81.73	0.45	30.25	43.52	24.33	0.05	0.07	0.61	0.60	Coarse sand, very well sorted, very fine skewed, very platykurtic
Site-8 Right bank (l=100cm)	25.69	81.72	10.46	36.75	41.58	11.22	0.85	0.70	0.41	2.78	Coarse sand, very well sorted, very fine skewed, very leptokurtic

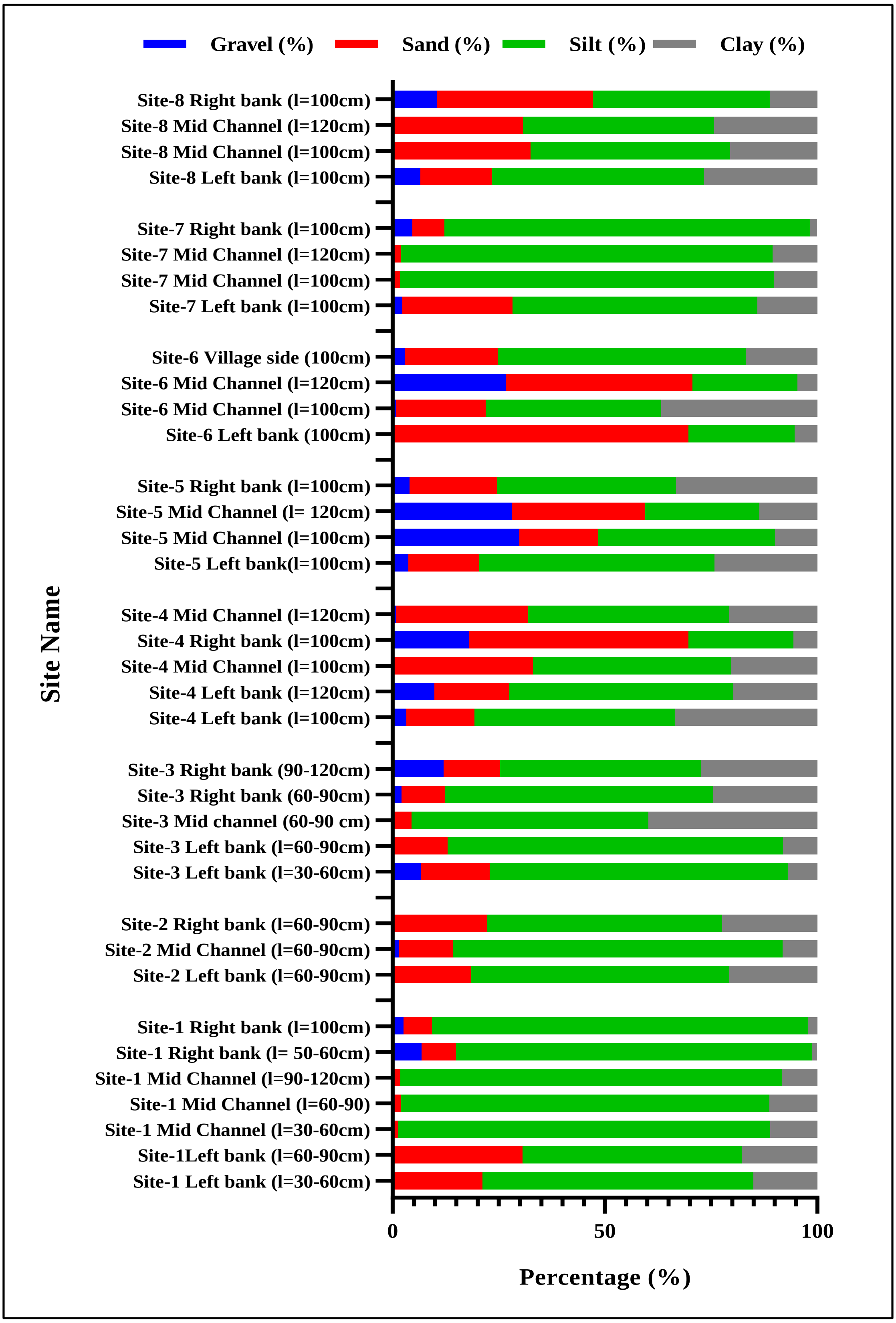

Fig. 5.12 Proportion of gravel, sand, silt, and clay in soil from left bank, middle of channel and the right bank.

5.3.4 Hydro-geomorphological Characterisation

The various geomorphological parameters such as sinuosity index, average width, radius of curvature, angle of curvature and bend tightness index of the delineated prominent channels and the traces of channels in the study area are worked out and are shown in Table 5.4. The sinuosity index of channels in Reach-1, Reach-2, Reach-3, and Reach-4 are 2.38, 3.11, 2.31, and 1.95, respectively (Table 5.4). The average sinuosity index of the delineated channel is 2.43 (Table 5.4). The total number of meanders in four reaches is about 82. The three selected meanders from each reach are named ‘1a,1b,1c; 2a,2b,2c; 3a,3b,3c; and 4a,4b,4c (marked by red colour in Fig. 5.9). The average width, radius of curvature, angle of curvature (AoC) and tightness index of the delineated channel are 164m, 5350.5m, AoC=123°, and 3.39 respectively (Table 5.4).

Table 5.4 Shows the parameters of the hydro- geomorphological features.

Reach	Channel Length(m)	Valley Length(m)	Sinuosity Index	Meanders Name	Width (W) (m)	Radius of Curvature (Rc) (m)	Angle of Curvature (AoC) (°)	Bend Tightness Index (Rc/W)
Reach-1	153583	64620	2.38	1a	144	238.65	AoC=112°	1.66
				1b	152	379.29	AoC=103°	2.50
				1c	137	284.05	AoC=135°	2.07
Reach-2	142071	45730	3.11	2a	141	445.67	AoC=87°	3.16
				2b	160	881.16	AoC=112°	5.51
				2c	112	500.51	AoC=145°	4.47
Reach-3	88995	38584	2.31	3a	243	586.11	AoC=150°	2.41
				3b	254	493.57	AoC=120°	1.94
				3c	277	1224.2	AoC=143°	4.42
Reach-4	85160	43629	1.95	4a	136	322.28	AoC=128°	2.37
				4b	107	550.26	AoC=120°	5.14
				4c	103	514.75	AoC=127°	5.00
Average			2.43		164	5350.5	AoC=123°	3.39

5.3.5 Optically Stimulated Luminescence (OSL) dating

The OSL ages of the sediment samples performed in TL/OSL (thermoluminescence and Optically Stimulated Luminescence) Laboratory, Wadia Institute of Himalayan Geology (WIHG), Dehradun, Uttarakhand, India, are presented in Table 5.5. The CAM (Central Age Model) age of sediments from the paleochannel site-1 is 1.2±0.2 ka. Since the overdispersion for the sediment from site OSL-1 (1.5m) and site OSL-2 is more than 15, MAM (Minimum Age Model) age was resorted to. Minimum Age Model (MAM) estimates the minimum age of the sample by assuming that the luminescence signal has been completely reset to zero during the last sunlight exposure. The calculated age represents the time since the last resetting event. Central Age Model (CAM) aims to find the central or most likely age of the sample. It considers the entire luminescence signal and calculates the age that best fits the data. CAM is often used when the luminescence signal shows complex behaviour. Depth (m): This represents the depth at which the sediment sample was taken from the channel. It is crucial in understanding the stratigraphy and depositional history of the sediment. U (ppm), Th (ppm), K (%): These values represent the concentrations of Uranium, Thorium, and Potassium in the sediment, respectively. These elements are important because they contribute to the natural radioactivity of the sediment, and their decay products are responsible for the luminescence signals used in OSL dating. Cosmic Dose rate (μGy/a): This is the dose rate contributed by cosmic radiation to the sediment. Cosmic radiation can ionize minerals, and the resulting trapped electrons contribute to the luminescence signal. Over dispersion (%): Over dispersion is a measure of the variability in the luminescence signal within the sample. Higher values may indicate incomplete signal resetting or mixing of different sediment components. Dose Rate (mGy/a): This is the total dose rate received by the sediment, considering contributions from natural radioisotopes (U, Th, K) and cosmic radiation. It's a crucial parameter for calculating the age of the sample in OSL dating. The MAM age of sediments from site OSL-1 (1.5m) and site OSL-2 are ‘1.3±0.1 and 0.3±0.02, respectively. Table 5.5 shows the various data details, such as the radioactive concentrations of U, Th, and K in the sediments, dose rate, paleo doses, and computed ages.

Table 5.5 Shows the OSL dating of sediment from the channel at two sites.

Sr. No.	Field no.	Depth (m)	U (ppm)	Th (ppm)	K %	Cosmic Dose rate (μGy/a)	Over dispersion (%)	Dose Rate (mGy/a)	CAM Age (ka)	MAM Age (ka)
1	Site-1, (1m)	1±0.1	4.22±0.4	16.3±1.6	3.0±0.3	174±17	12±2	5.11±0.3	1.2±0.2	Nil
2	Site-1, (1.5m)	1±0.1	3.87±0.3	23.6±2	2.8±0.3	167±16	25±3	5.07±0.3	1.6±0.4	1.3±0.1
3	Site-2, (1.5m)	1.5±0.1	12.54±1.2	20.9±2	3.0±0.3	167±16	46±8	7.2±0.4	0.6±0.3	0.3±0.02

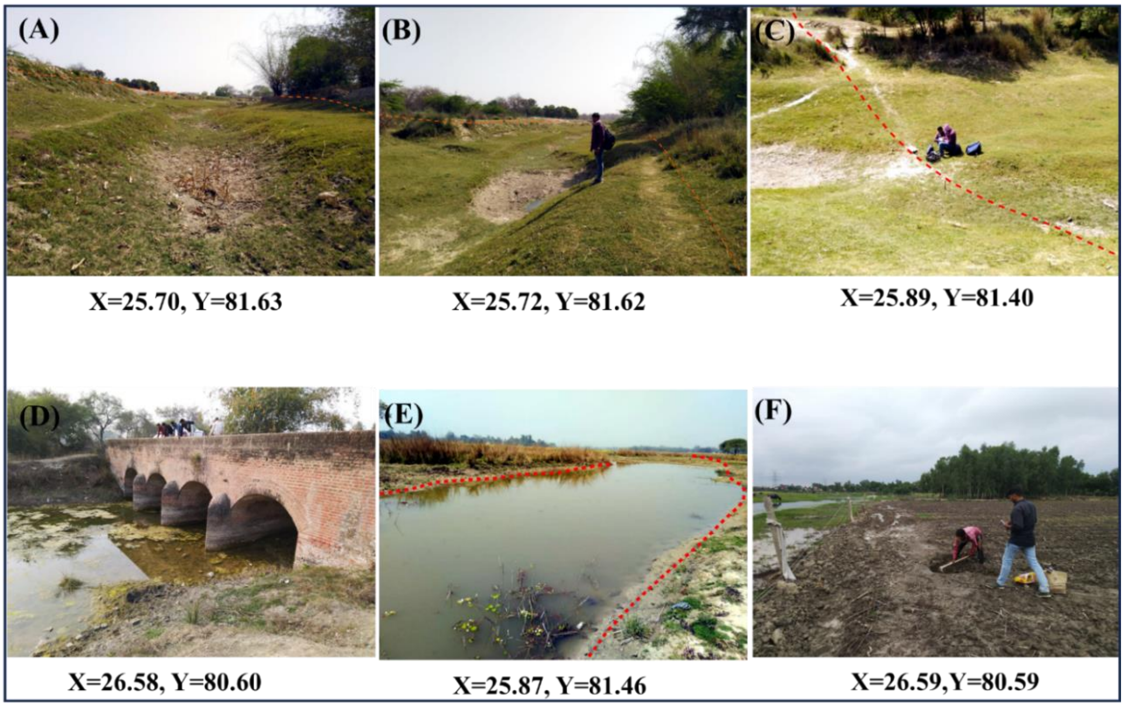

Fig. 5.13 Field photographs: (A) and (B) show the paleochannels, (C) Red line in the photograph shows the line (across the paleochannel) along which the resistivity survey has been carried out. (D) and (E) photographs show the prominent channels, and (F) Sites from which samples have been taken for the OSL dating. The latitude and longitude of each photograph are shown by X and Y, respectively.

5.4 Discussion

1. Remote sensing data (Landsat-8 OLI satellite image, SRTM DEM) revealed a system of numerous sinuous underfit rivers, paleochannels, and associated ox-bow lakes and meander scars over the tract of about 200km long in the interfluvial zone of the Ganga and Sai Rivers. Band enhancement of satellite images helped in the general identification and delineation of these geomorphic features, which outlined geomorphic characteristics based on the pattern of water bodies (oxbow-lakes, scrolls, etc.) and human settlements through careful observation and interpretation. Despite the gross delineation of the possibly connected segments, there are still some gaps, which are not visualised in the satellite image and, thus, superimposition of DEM data, supplemented to accurately decide the past route. DEM data well corroborated the delineated underfit rivers, paleochannels and associated oxbow lakes, as these geomorphic features were visualised in a dark tone in the DEM map. The geomorphological parameters (Fig. 5.10 and Table 5.4) show that the pattern and orientations of these numerous sinuous underfit rivers, paleochannels, and

associated ox-bow lakes and meander scars are highly variable, and they represent convexity (or concavity) in all possible directions. They are mostly curvilinear but also sharply bent or completely looped with or without angular turnings. The continuity of these delineated underfit rivers, paleochannels (orange coloured in Fig. 5.5) and associated oxbow lakes (green coloured in Fig. 5.5) in the upper tract as well as in the lower tract with the currently flowing Bakulahi river course (Blue coloured stream in Fig. 5.5) reveal that they are integral parts of Bakulahi River.

2. The Bakulahi River actually originated in the interfluvial tract from Gouria Kalan village near Bangarmau in the Unnao district. Flowing through 3 districts (Unnao. Raibareli, and Pratapgarh), it meets the Sai River at Khajurni village in the Pratapgarh district. The total length of the channel course of the Bakulahi, with several disconnected channels/streams of Bakulahi, is 558 km, and its average width is 150 m.

3. In spite of corroboration between the satellite image and DEM data, the outcomes of the DEM studies may be quite misleading as they generate flow paths with an extraordinary number of streamlets for the scatter of undulations, which is not true for floodplain geomorphology. Therefore, field observations and geophysical surveys such as resistivity profiling are required for confirmation. In order to ascertain the beginning of the Bakulahi River, the uppermost recognisable channel features in the alignment near Asarfabad village and near Dholwa village (Unnao) were studied. The first appearance of traces of two isolated meanders was important to decipher if they belonged to the same continuous channels. The spatial cross-sectional profiles of the traces of these two isolated meanders and other traces of channels at four different sites (recognized in remote sensing data) generated from SRTM DEM data give the U or V-shaped transverse forms and dimensions (Fig. 5.11). Further, the decrease in resistivity value across these traces of channel (recognized in remote sensing data) (Fig. 5.11) is due to the presence of moisture condition which reveal about the presence paleochannels. Since the traces of channel shows continuity with the Bakulahi River channel and the moisture condition across the traces of channel distributed over the same width as the Bakulahi River channel, we can say these traces of channels are the part of the Bakulahi River. All the segments successively join to make the lost stream of the Bakulahi River over the approximately 200 km tract.

4. The grain size analysis conducted along the Bakulahi River's course has unveiled critical insights into its behaviour and historical evolution. The distribution of sediment, ranging from silt loam to silty clay loam and silt, reflects the complex interplay of kinetic energy variations from the central channel to the banks. Examination of segmented river courses reveals distinct phases of flow, with older courses featuring sandy-levee built banks indicating higher energy states, while sandy silt in the last phase signifies a migratory flow pattern. Directional continuity between older and self-built courses suggests influence from previous river paths. Additionally, grain size distributions show spatial variability in energy states, while studies suggest the river's independence from neighbouring rivers' bank formation processes. Optically Stimulated Luminescence (OSL) dating indicates the river's age to be older than 1.3±0.1 ka, underlining its long history of lateral shifting and geomorphological evolution.

5. The hydro-geomorphological parameters conclude that the Bakulahi River illustrates a pronounced tendency for rapid changes in the river course, primarily attributed to highly sinuous bends. The relationship between W and Rc helps to predict that the river channel is highly instable, exhibiting a more pronounced tendency for migration through meander loop cut-offs rather than lateral migration. These findings underscore the river's unpredictable and erosive nature, reflecting an inherent inconsistency in its behaviour.

6. Since the quaternary period, tectonic activity and climate have significantly controlled the river morphology in the Gangetic plains. The remote sensing image shows that near Gauriya Kalan village (Unnao), the Bakulahi River was possibly affected by the Sandila fault (Singh et al. 2006). It might be possible that due to the Sandila fault water in the Bakulahi River became blocked and distracted and further, due to low flow energy and intermittent high sedimentation load Bakulahi River lost its course continuity and finally become extinct. A system of ox-bow lakes, meanders, relict fluvial features, and complex scrolls formed around the Bakulahi River, have undergrown through erosion and depositional processes to generate shallow water bodies and eventually converted into riverine wetlands. Presently, the whole area is as ecologically and environmentally indispensably important and valuable that the two riverine wetlands are considered as Ramsar sites.

5.5. Conclusion

1. This study shows a continuous and properly interconnected paleochannel and the series of associated ox-bow lakes and meanders of the Bakulahi River in the interfluvial zone of the Ganga and Sai Rivers. The currently flowing Bakulahi River actually originated from Gouria Kalan village near Bangarmau in the Unnao district. Flowing through 3 districts (Unnao. Raibareli, and Pratapgarh), it meets the Sai River at Khajurni village in the Pratapgarh district. The total length of the channel course of the Bakulahi, with several disconnected channels/streams of Bakulahi, is 558 km, and its average width is 150 m.
2. The spatial cross-sectional profiles generated from SRTM DEM data give the U or V-shaped transverse forms and dimensions of the paleochannel of the Bakulahi River. The geophysical survey confirms the continuity of paleochannels in those parts where the continuity of the paleochannel cannot be visualised in satellite images.
3. The geomorphology and sedimentological analysis of Bakulahi River presents a specific stage of the river in flood plains, which has lost the continuity of its channel course and its continuous flow. It shows two important signatures: firstly, the self-burying of its course by its own sediment load and secondly, the obliteration of parts of its course and complete looping of courses with angular turnings. These characteristics are associated on both sides with abnormal bending and turning. Owing to the effect of neo-tectonism, the river underwent a decrease in its mass, and therefore, energy could not survive its course, and became extinct. Later on, a system of ox-bow lakes, meanders, relict fluvial features, and complex scrolls eventually converted into riverine wetlands. Presently, there are two Ramsar sites associated with the riverine wetland system. The OSL dating infers that the Bakulahi River might be older than 1.3±0.1 ka.
4. Extensive deforestation in the upper tract leads to high sediment yield and change in hydrograph. The influx of sediment from higher-level flood plain from both sides of the Bakulahi River and flood accretion deposits of the Ganga and Sai limiting the interfluvial tract reduced the available area for Bakulahi sediments to deposits laterally and led to chocking of its own course. Any planning regarding the rejuvenation of the Bakulahi River should follow the entire path as deciphered in this work, which does not show continuity as a flowing river or continuous channel.